CFD Simulation and Experimental Study of a Parabolic Trough Collector Alternative

Qussay Hroub
LASEM Laboratory, ENIS, University of Sfax
Sfax, Tunisia
qusai.o.m.hroub@gmail.com

Youssef Drira
MAI Laboratory, ENIT, Tunis El Manar University
Tunis, Tunisia
youssefdrira@gmail.com

Skander Jribi
LASEM Laboratory, ENIS, University of Sfax
Sfax, Tunisia

Hatem Bentaher
LASEM Laboratory, ENIS, University of Sfax
Sfax, Tunisia

2022 13th International Renewable Energy Congress (IREC) | 978-1-6654-8897-6/22/$31.00 ©2022 IEEE | DOI: 10.1109/IREC56325.2022.10002125

***Abstract*— Concentrated solar thermal (CST) systems require high manufacturing technology and expensive costs which explain their low adoption in developing countries. In a search for more affordable CST, parabolic trough collector with stainless steel sheet (PTC-SS) seems to be a good alternative. In this study, the PTC-SS performance were evaluated using optical and thermal studies. The optical evaluation was carried out by simulating the PTC-SS on Soltrace software and the thermal evaluation was conducted by simulating the PTC-SS receiver on Ansys software. Additionally, the simulation results have been validated by comparing the amount of heat gained by the water between the simulation and the experiment. The results show that the heat gained by the water was approximately 502.6 W. The simulation results were 33.32% higher comparing to experimental data. Finally, further studies to evaluate the PTC-SS overall performance will be carried out.**

Keywords—CST; PTC-SS; CFD; Renewable energy

I. INTRODUCTION

The world's need for energy and power has significantly increased as a result of population growth, industrialization, and urbanization. [1]. Solar energy is one of the most competitive options among all energy sources, simply because it is renewable and sustainable [2].

Concentrated solar thermal (CST) technologies have been used in many applications such as industrial heat, desalination, chemical processes, solar cooling, and electricity production [3]. The most common technology is the parabolic trough collector (PTC) [4]. However, due to the high cost and complexity of this technology, various studies are looking into alternative designs [5].

Since the solar collecting system performance depends on the efficiency of the sunlight collection, the alternatives research field has led to the development and introduction of new materials which have different properties. Currently, these new materials that are commercially available provide a challenge because their properties are more complex [6].

The aim of this research is to evaluate the performance of the proposed alternative; PTC with stainless steel sheet (PTC-SS) as a reflector. Using an evacuated tube with U pipe as a receiver, this evaluation will have an optical analysis by simulating the PTC-SS on Soltrace software and a thermal analysis by simulating the PTC-SS receiver on Ansys software then validation will be carried out with experimental data.

II. METHODOLOGY

A. PTC-SS Design

The PTC-SS has two main parts; reflector and receiver. The reflecting part is a stainless-steel sheet following a parabolic shape. This geometric shape allows it to concentrate the sun's rays in a focal line. In this line, a receiver containing the working fluid is placed. Fig. 1 shows the PTC-SS parts.

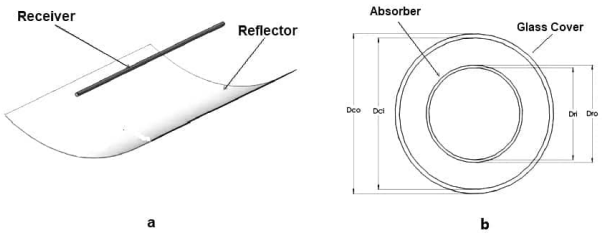

Fig. 1. PTC-SS parts.

The receiver is a double glass tube surrounding a copper U pipe. The double glass tube contains a vacuum space in order to reduce heat losses. The outer glass is transparent that allowing the incident rays to pass through it. The inner glass is painted with a selective coating (The absorber) that absorbs these rays. Within this double glass, a U pipe collected the heat and transfers it to the working fluid (water). The U pipe is fixed inside the glass tube with an aluminum fin [7]. Fig. 2 shows the receiver characteristics.

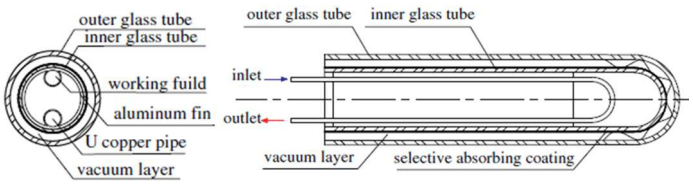

Fig. 2. The receiver components [7].

A small-scale prototype was created to evaluate the performance of the PTC-SS [8]. Using basic materials, this prototype was created with the listed dimensions in Table 1.

978-1-6654-8897-6/22/$31.00 ©2022 IEEE

Authorized licensed use limited to: Institut Teknologi Sepuluh Nopember. Downloaded on September 08,2026 at 05:43:51 UTC from IEEE Xplore. Restrictions apply.

B. Experiment Setup

An Experiment has been carried out on February 5th, 2022 between 11:00 and 16:30 in the LASEM laboratory at the National School of Engineers of Sfax. The PTC-SS collecting system was a closed system with a 12 L water tank. The water is circulated by a pump passing through the U pipe to be heated then returns to the tank.

The sun was manually tracked on a single axis. Pt100 sensors were used to measure the water temperature at the inlet and outlet of the receiver and inside the tank. Direct solar radiation was measured using a pyranometer. All these devices were connected to a data logger.

Ambient temperature and wind speed were measured using an anemometer. Fig. 3 presents the PTC-SS collecting system.



Fig. 3. PTC-SS collecting system.

The experiment conditions change dynamically throughout the day, especially the weather conditions. To simplify this experiment, we chose to study the collected data in the midday period since most conditions variate slightly in this period thus it may be assumed as a steady state period.

The ambient temperature average was around 24°C. Wind speed was approximately 0.3 m/s. The direct normal irradiation in the midday period was around 700 W/m². The water flow rate was 0.03 kg/s, entering the U pipe with a temperature of 50°C.

C. Governing Equations of PTC-SS

The general governing equations for the Finite Volume Method (FVM) model of the entire receiver in the Fluent-code include the continuity, momentum, energy equations and the standard $k-\varepsilon$ two-equation turbulence model [9]. These equations can be expressed as follows:

Continuity equation:

$$\frac{\partial}{\partial x_i}(\rho u_i) = 0 \tag{1}$$

Momentum equation:

$$\frac{\partial}{\partial x_i}\left(\rho u_i u_j\right) = -\frac{\partial p}{\partial x_i} + \frac{\partial}{\partial x_j}\left[(\mu_\mathrm{t} + \mu)\left(\frac{\partial u_i}{\partial x_j} + \frac{\partial u_j}{\partial x_i}\right) - \frac{2}{3}(\mu_\mathrm{t} + \mu)\frac{\partial u_l}{\partial x_l}\delta_{ij}\right] + \rho g_i \tag{2}$$

Energy equation:

$$\frac{\partial}{\partial x_i}(\rho u_i T) = \frac{\partial}{\partial x_i}\left[\left(\frac{\mu}{\mathrm{Pr}} + \frac{\mu_\mathrm{t}}{\sigma_\mathrm{T}}\right)\frac{\partial T}{\partial x_i}\right] + S_\mathrm{h} \tag{3}$$

k equation:

$$\frac{\partial}{\partial x_i}(\rho u_i k) = \frac{\partial}{\partial x_i}\left[\left(\mu + \frac{\mu_\mathrm{t}}{\sigma_\mathrm{k}}\right)\frac{\partial k}{\partial x_i}\right] + G_\mathrm{k} - \rho\varepsilon \tag{4}$$

Ɛ equation:

$$\frac{\partial}{\partial x_i}(\rho u_i \varepsilon) = \frac{\partial}{\partial x_i}\left[\left(\mu + \frac{\mu_\mathrm{t}}{\sigma_\varepsilon}\right)\frac{\partial \varepsilon}{\partial x_i}\right] + \frac{\varepsilon}{k}(c_1 G_\mathrm{k} - c_2\rho\varepsilon) \tag{5}$$

where the turbulent viscosity μ_t is given by:

$$\mu_\mathrm{t} = C_\mu \rho \frac{k^2}{\varepsilon} \tag{6}$$

G_k denotes the production rate of k and is given by:

$$G_\mathrm{k} = \mu_\mathrm{t}\frac{\partial u_i}{\partial x_j}\left(\frac{\partial u_i}{\partial x_j} + \frac{\partial u_j}{\partial x_i}\right) \tag{7}$$

The standard constants are C_μ = 0.09, c_1 = 1.44, c_2 = 1.92, σ_k = 1.0, σ_ε = 1.3, σ_T = 0.85 [10].

In the above equations, ρ is the density (kg/m^3); u is the velocity component (m/s); x cartesian coordinate (m); p is the pressure (Pa); μ is the dynamic viscosity (Pa.s); μ_t is the turbulent dynamic viscosity; g is the gravity (9.801 m/s^2); T is the temperature (K); Pr is the Prandtl number; σ_T is the turbulent Prandtl number; S_h is the source term (W/m^3); k is the turbulent kinetic energy (m^2/s^2); ε is the turbulent dissipation rate (m^2/s^3); c_1 and c_2 are the coefficients in turbulence model [11].

D. Soltrace Simulation

The PTC-SS reflector redirects sun's rays to be collected by the receiver creating a non-uniform heat flux (HF) distribution on the absorber surface [12]. The PTC-SS performance is influenced by the HF distribution on the PTC-SS absorber [13]. Therefore, the geometric shape and optical parameters (OP) of PTC-SS plays an important role in the distribution shape [8]. Due to this great role, it will be used on Soltrace software to evaluate the PTC-SS optical behavior and to get the closest HF distribution to reality [13]. The simulation of the HF distribution on Soltrace is carried by considering the PTC-SS dimensions and OP as shown in Tables 1 and 2. The sun was simulated with Gaussian distribution with a 2.6 mrad cone angle [8] and for the direct normal irradiation we will use the experimental data for all simulations.

E. Ansys Simulation

In order to evaluate the thermal effect of the flux distribution on water, the PTC-SS receiver was simulated on Ansys.

Authorized licensed use limited to: Institut Teknologi Sepuluh Nopember. Downloaded on September 08,2026 at 05:43:51 UTC from IEEE Xplore. Restrictions apply.

However, the existence of the vacuum space reduces the convection and conduction losses, thus these losses can be neglected. Therefore, this simulation was carried out by creating a geometric model starting with the absorber. Then, an appropriate mesh was applied to this model. Fig. 4 shows the Absorber meshing.

TABLE I. PTC-SS DIMENSIONS

Parameter	Value	Unit
Inner/outer glass diameter	48/58	mm
Absorber length	1700	mm
Internal/External Diameter of U copper pipe	6/8	mm
PTC-SS width	1500	mm
PTC-SS length	1700	mm
Concentration ratio (CR)	9.56	-
Focal length	314.66	mm
Rim angle	100	°

TABLE II. PTC-SS OPTICAL PARAMETERS

Parameter	Value
Stainless steel sheet reflectivity	0.8
Transmittance of the outer glass	0.9
Absorptance of the selective coating	0.9
Intercept factor	0.8

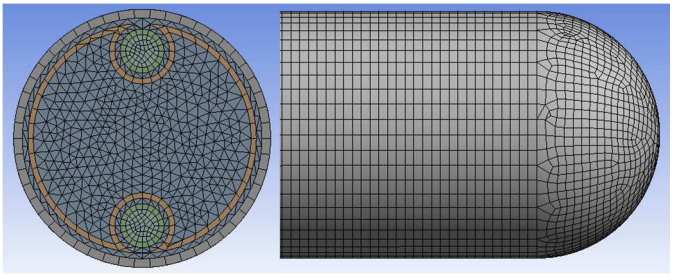

Fig. 4. Absorber meshing.

For the setup step we used a Pressure-Based solver with steady time and absolute velocity formulation also the energy and standard k-epsilon viscous models were enabled, then the absorber's materials (glass, aluminum, copper, air, and water) were defined.

As for the boundary conditions, the water flow rate and inlet temperature with the values noted in the experiment were applied to the water inlet.

Fig. 5 shows the water boundary conditions. To apply heat flux on the surface of the absorber, the obtained flux distribution from Soltrace simulation results was used by converting it into a user-defined function (UDF). Fig. 6 shows the heat flux boundary condition.

As for the solution we choose “SimpleC scheme” method and second order for all spatial discretization. Moreover, the hybrid initialization method was used.

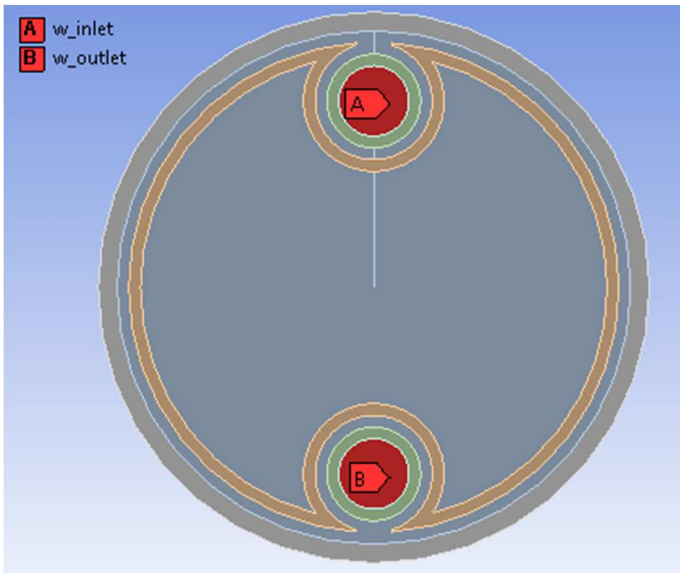

Fig. 5. The water boundary conditions.

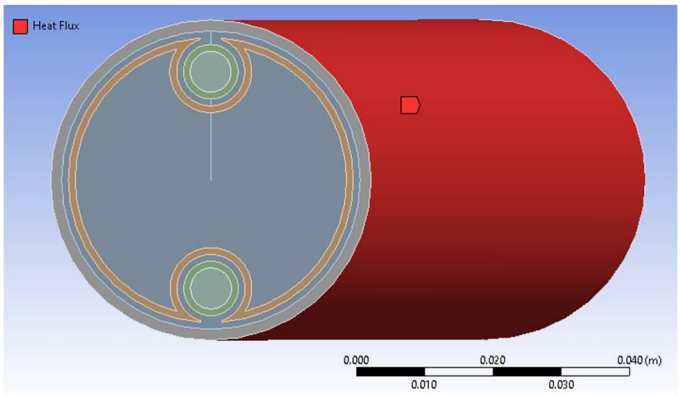

Fig. 6. The heat flux boundary condition.

To validate the simulation with experiment we will compare the amount of heat gained by the water for the results of both of them. The heat gain can be calculated by [14]:

$$Q = \dot{m}\, c_p\, (T_o - T_i) \quad (8)$$

Where (T_i) and (T_o) are the inlet and outlet temperatures in kelvin (K), ($\dot{m}$) is the water mass flow rate (kg/s) and (c_p) is the water specific heat (J/(kg.K)).

III. RESULTS AND DISCUSSION

A. *Soltrace Results*

Fig. 7 shows the solar radiation variation during the midday period. The radiation average was about 700 W/m² with a maximum variation near to 10 W/m². Fig. 8 shows the results of using this data in Soltrace. The HF distribution on the glass cover circumferential angle was symmetric also it shows that the PTC-SS collected an average flux of 6930 W/m². This average without considering the listed optical parameters (OP) in table 2 (The flux average before passing through the glass cover).

PTC-SS have a maximum HF for circumferential angles -106.5° and 111° which means that both sides of the absorber collected more solar rays.

Authorized licensed use limited to: Institut Teknologi Sepuluh Nopember. Downloaded on September 08,2026 at 05:43:51 UTC from IEEE Xplore. Restrictions apply.

Fig. 8 also shows the heat flux (HF) distribution on the absorber circumferential angle (after taking the OP into account). The PTC-SS absorber collected an average flux of 3590 W/m² with the same distribution.

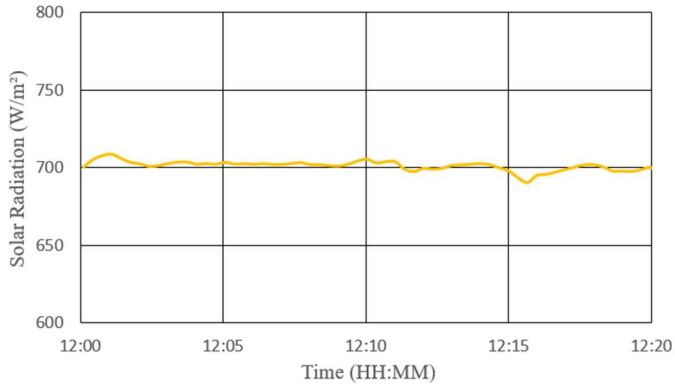

Fig. 7. Solar radiation variation during the midday period.

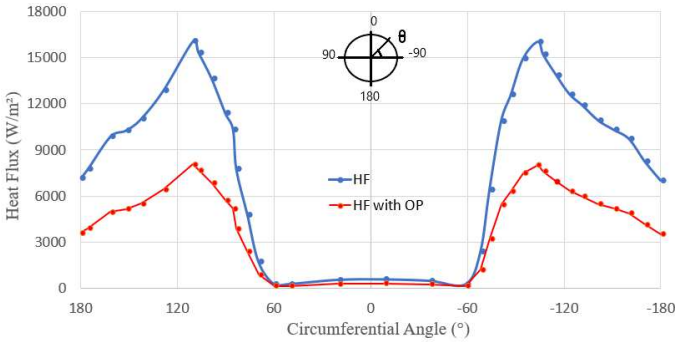

Fig. 8. The heat flux distribution curve.

B. *Ansys Results*

The flux distribution in figure 8 with an average of 3590 W/m² leads to a similar temperature distribution on the absorber. Fig. 9 shows the temperature distribution on the absorber surface.

The HF distribution applied to the absorber leads to a similar heat distribution on the U pipe surface. The average of power that has reached the U pipe was 502.6 W. Fig. 10 shows the flux distribution on the U pipe.

The difference between inlet and outlet temperature in simulation results during the midday period was 4 degrees which leads to heat gain around 502.2 W.

C. *Experiment Data*

Fig. 11 shows the water temperature in the U pipe inlet and outlet during the midday period. As noted in this figure the water temperature in the experiment was increased by around 3 degrees at the end of this period.

Also, in figure11 we can see that the difference between the water inlet and outlet temperature in both of the experiment and simulation was always constant and the curves are behaving in the same way.

Fig. 12 shows the difference between inlet and outlet temperature during the midday period. For the experiment, this difference remained at the value of 3 degrees during this period which leads to heat gain around 376.7 W.

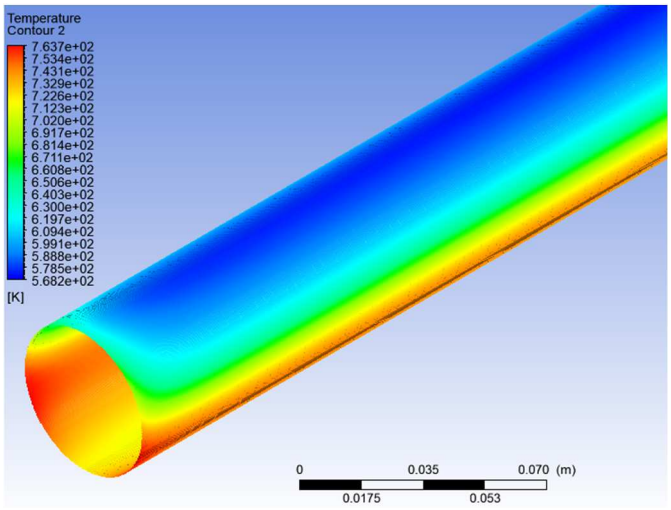

Fig. 9. The temperature distribution on the absorber.

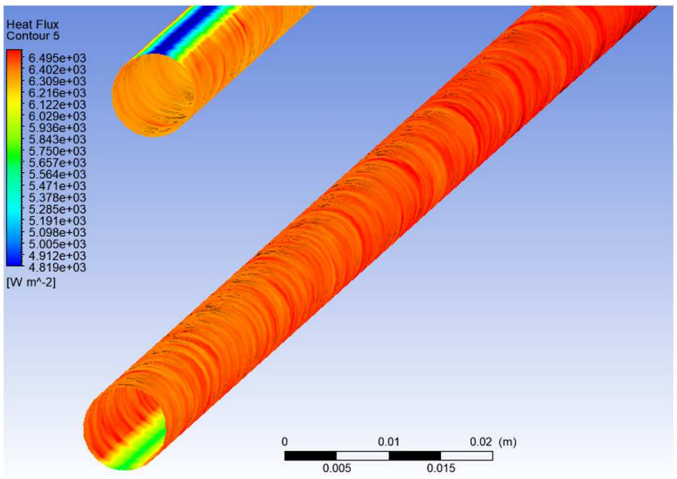

Fig. 10. The flux distribution on the U pipe.

Furthermore, we can notice that the blue points which represent experimental data are not line up in the same way as the simulation results represented by the red line. This might be happening as a result of two reasons; the solar radiation variation and the sun tracking errors. If we take a look back to figure7, we can see that the solar radiation variation is affecting the water temperature in the same way, especially in the second half of the period. As for the first half according to figure7, the water temperature in figure.12 should be higher than what was recorded. As we described earlier in the experiment setup our sun tracking system was a manual system. Therefore, the temperature drops in the first half of the experience period caused by sun tracking errors. Actually, the tracking system should be improved to avoid any unexpected drop in water temperature.

In the experiment results, the water gained an average of heat around 376.7 W. While the water gained an average of heat around 502.2 W in the simulation results. The difference between the experiment and simulation was approximately 125.5 W. The simulation was 33.32% higher. This difference

Authorized licensed use limited to: Institut Teknologi Sepuluh Nopember. Downloaded on September 08,2026 at 05:43:51 UTC from IEEE Xplore. Restrictions apply.

caused by the existence of thermal losses which we considered equal to zero in the CFD pre-processor.

Thus, to reduce the gap between simulation and experiment, the assumption of the thermal losses absence due to vacuum space should be modified. The reduction of the thermal losses can be achieved by reducing the receiver layers or by replacing them with materials with better thermal conductivity.

Moreover, the assumption of the thermal losses absence due to vacuum space should be modified by studying the PTC-SS thermal properties more in detail. Also, the sun tracking system should be improved to avoid any unexpected drop in water temperature.

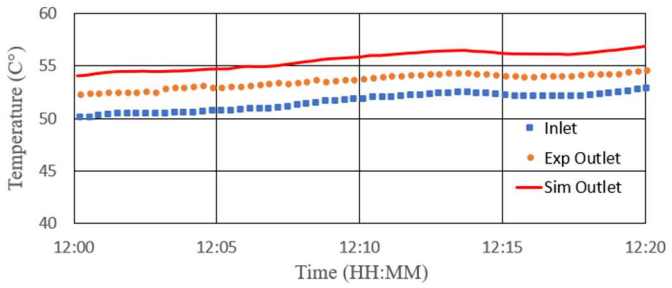

Fig. 11. Water temperature at the inlet and outlet during the midday period.

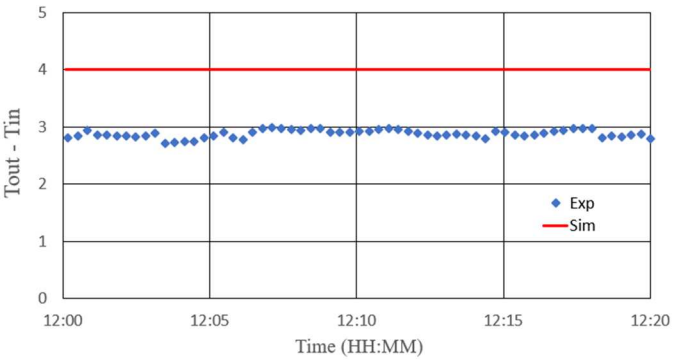

Fig. 12. The difference between water temperature at the inlet and outlet.

IV. Conclusions and Perspectives

In this paper, an experimental and a simulation studies of a Parabolic Trough Collector (PTC) alternative were carried out. The optical simulation of the PTC with a stainless-steel sheet (PTC-SS) was performed using Soltrace software to obtain the non-uniform heat flux on the receiver. For a solar radiation of 700 W/m^2, PTC-SS collected an average flux of 6930 W/m^2. Considering the optical parameters of the receiver and reflector, the average heat flux reaching the U-pipe was only 3590 W/m^2. The latter distribution on the U-pipe was used as a boundary condition in the CFD software. The simulation results showed that the receiver gained 502.2 W. The difference of heat gain between the simulation and experiment was approximately 125.5 W which corresponds to 33.32% of the simulated power output. This difference was mainly caused by thermal losses.

References

[1] M. T. Islam, N. Huda, A. B. Abdullah, and R. Saidur, 'A comprehensive review of state-of-the-art concentrating solar power (CSP) technologies: Current status and research trends', Renewable and Sustainable Energy Reviews, vol. 91, pp. 987–1018, 2018.

[2] S. A. Kalogirou, 'Solar thermal collectors and applications', Progress in Energy and Combustion Science, vol. 30, no. 3, pp. 231–295, 2004.

[3] S. Mekhilef, R. Saidur, and A. Safari, 'A review on solar energy use in industries', Renewable and Sustainable Energy Reviews, vol. 15, no. 4, pp. 1777–1790, 2011.

[4] B. Zou, Y. Jiang, Y. Yao, and H. Yang, 'Optical performance of parabolic trough solar collectors under condition of multiple optical factors', Applied Thermal Engineering, vol. 160, p. 114070, 2019.

[5] E. Bellos and C. Tzivanidis, 'Alternative designs of parabolic trough solar collectors', Progress in Energy and Combustion Science, vol. 71, pp. 81–117, 2019.

[6] A. Gagliano, F. Nocera, F. Patania, and A. Contino, 'A procedure for the characterization of the solar-weighted reflectance of mirrored reflectors', in 2014 5th International Renewable Energy Congress (IREC), hammamet, Tunisia, Mar. 2014, pp. 1–6.

[7] Y. Gao et al., 'Thermal performance and parameter analysis of a U-pipe evacuated solar tube collector', Solar Energy, vol. 107, pp. 714–727, 2014.

[8] Y. Drira et al., 'Error Optimization of Semi-Parabolic Linear Fresnel Reflector', in 2021 12th International Renewable Energy Congress (IREC), Hammamet, Tunisia, Oct. 2021, pp. 1–5.

[9] T. Echekki and E. Mastorakos, Eds., Turbulent Combustion Modeling, vol. 95. Dordrecht: Springer Netherlands, 2011.

[10] Y.-L. He, J. Xiao, Z.-D. Cheng, and Y.-B. Tao, 'A MCRT and FVM coupled simulation method for energy conversion process in parabolic trough solar collector', Renewable Energy, vol. 36, no. 3, pp. 976–985, Mar. 2011.

[11] O. García-Valladares and N. Velázquez, 'Numerical simulation of parabolic trough solar collector: Improvement using counter flow concentric circular heat exchangers', International Journal of Heat and Mass Transfer, vol. 52, no. 3–4, pp. 597–609, Jan. 2009.

[12] W. Peng and O. K. Sadaghiani, 'Evaluation of Heat Flux Distribution Uniformity around the Receiver Tube of Parabolic Trough Collector based on Six Statistical and Geometrical Indices', International Journal of Heat and Mass Transfer, vol. 164, p. 120547, 2021.

[13] Y. Drira, N. Fakhfakh, S. Jribi, H. Bentaher, I. Benhassine, and L. Ammar, 'Performance Investigation of Solar Parabolic Trough Collector Alternatives', Arab J Sci Eng, Nov. 2022.

[14] Jaramillo, O.A., Venegas-Reyes, E., Aguilar, J.O., Castrejón-García, R., Sosa-Montemayor, F., 2013. Parabolic trough concentrators for low enthalpy processes. Renewable Energy 60, 529–539.

Authorized licensed use limited to: Institut Teknologi Sepuluh Nopember. Downloaded on September 08,2026 at 05:43:51 UTC from IEEE Xplore. Restrictions apply.